Biomass Conversion and Biorefinery (2023) 13:10483–10494
https://doi.org/10.1007/s13399-021-01741-1

ORIGINAL ARTICLE

Immobilized ZnO/TiO_2 activated carbon (I ZnO/TiO_2 AC) to removal of arsenic from aqueous environments: optimization using response surface methodology and kinetic studies

Nastuna Ghanbari Sagharloo[1] · Mohammad Rabani[1] · Lida Salimi[1] · Hossein Ghafourian[1] · S. M. T. Sadatipour[1]

Received: 10 June 2021 / Revised: 22 June 2021 / Accepted: 3 July 2021 / Published online: 19 July 2021

Abstract
Removal of arsenic (As), as a toxic, carcinogenic, and mutagenic water pollutant, has been a topic of much thought and discussion within environmental experts newly. One of the most popular AS removal method from aqueous solution is adsorption. To the best of our knowledge, the combination of ZnO/TiO_2 immobilized on activated carbon (AC) has not been used to AS removal from water. Therefore the aims of this study are (i) to develop a novel immobilized ZnO/TiO_2 activated carbon (I ZnO/TiO_2 AC) for effective and economic arsenic removal, (ii) to investigate the effects of different variables (e.g., pH, contact time, dose) on I ZnO/TiO_2 AC system efficiency, (iii) to achieve nonlinear modeling using response surface methodology (RSM) approach, and (iv) to optimize I ZnO/TiO_2 AC system for As removal from water with RSM-based developed model**.** The final appropriate solution which was selected by developed response surface model demonstrated that the best dosage, pH, contact time, and initial concentration to reach permitted concentration for output (10 µg/L) are 5.187 g/L, 6.758, 287.574 min and 9.767 mg/L, respectively. The appropriate achieved desirability (0.996) depicted that the solution is acceptable.

Keywords Response surface methodology (RSM) · I ZnO/TiO_2 AC · Water · Arsenic · Photocatalyst · Adsorption

1 Introduction

Discharge from industry contains various organic and inorganic pollutants [1–3]. Among these pollutants are heavy metals which can be toxic or carcinogenic and which are harmful to humans and other living species [4]. Removal of arsenic (As), as a toxic, carcinogenic and mutagenic water pollutant, has been a topic of much thought and discussion within environmental experts newly [5]. Industrial activities (e.g., mining), agricultural crop protection products (e.g., pesticides and herbicides containing As), natural events (e.g., forest fires), and fossil fuels combustion and so on have led to increasing in As level ranged between 0.1 and 230 mg/L in water and wastewater [6]. On the other hand, the As standard limitation guideline purposed by World Health Organization (WHO) and the US Environmental Protection Agency (USEPA) has become more strict (e.g., 0.01 mg/L for drinking water). Therefore, finding an effective, economic, and innovative solution for purification of water containing As is essential. There are different types of toxic heavy metals (e.g., As) treatment method including adsorption [7], precipitation [8], nanoparticles [9], membrane separation [10], electrocoagulation [11], ion exchange [12], and photo-catalyst [13–15]. Although these methods were reported useful to remove a wide variety of pollutants as well as As [16, 17], researchers have focused on finding more effective and economic techniques through coupling systems, novel method development, and other modifications [18–21] due to above-mentioned reasons. These efforts have led to development of some emerging processes for As

✉ Mohammad Rabani
mhd_rabani@yahoo.com

Nastuna Ghanbari Sagharloo
nasi_ghanbari@yahoo.com

Lida Salimi
salimilida@yahoo.com

Hossein Ghafourian
ghaforian25@yahoo.com

S. M. T. Sadatipour
sadatipour1960@yahoo.com

[1] Department of Environmental Engineering, Tehran North Branch, Islamic Azad University, Tehran, Iran

removal, but more try is needed to find a better solution. One of the most popular As removal method from aqueous solution is adsorption. Despite many advantages of adsorption such as treatment stability, simplicity of operation, and no need to chemicals, which make this process popular, serious modifications are required to overcome its drawbacks including desorption, relatively high cost, low selectivity, and slow adsorption kinetic rates. A possible approach in order to improve adsorption process is integrating it with a high tech effective method that can solve previous problems and make it as a novel practical technique. To achieve this different alternative are available and nano-photocatalysts (NP) seems to be the best choice because of its unique potential abilities. In terms of As removal, converting the As (III) to As (V) by photocatalytic oxidation can improve capability of adsorption system [22]. Besides, As can also be adsorbed by NP because of small size, large surface area, and multiple active sites [17] which enhance As removal. Thus the idea of combined use of photocatalyst and adsorbent for As removal was introduced by Nakajima et al. [23]. Their findings demonstrated that by using a combination of adsorbent and TiO_2 suspension, all types of As were converted into As (V), then very good As removal (~ 97%) was achieved by photocatalyst–adsorbent system. In another work, Zhang, Fu-Shen, and Hideaki Itoh were studied simultaneous photocatalytic-oxidation and adsorption of As using slag-iron oxide-TiO_2 adsorbent (adsorbent developed by solid waste slag, iron oxide, and TiO_2). The obtained results showed optimum condition pH = 3, adsorbent dose = 2 g/l (As concentration = 20 mg/L), and 5 g/l (As concentration = 50 mg/L) to oxidize and remove As from aqueous solution. They emphasized that photocatalyst makes developed adsorbent efficient and economic [24]. The effect of the crystalline size (6.6–30.1 6.6 and 30.1 nm) on photocatalytic oxidation and adsorption of As using TiO_2 NP were determined by Xu Zhonghou and Xiaoguang Meng [25]. They documented that although the rate of As (III) oxidation was not significantly affected by changes in NP size between 6.6 and 14.8, the oxidation rate decreased with an increase in particle size (14.8–30.1 nm). In all of this attempts, two major difficulties of this combined system are remain: (1) difficult and time-consuming NP separation from treated water and (2) high treatment cost which finding a solution for them is the main goal of this study. Among different type of NP, titanium dioxide (TiO_2) showed good photo-oxidation of As (III) to As (V) as well As adsorption [22]. There is a widespread tendency to utilize TiO_2 to water and wastewater treatment for its exclusive properties including non-toxicity, insolubility, and photostability [26]. To solve recovery (separation) difficulties of this NP, immobilization of TiO_2 on inert materials (e.g., activated carbon) and development of integrated photocatalytic adsorbent (IPAs) has been suggested [27]. In terms of resolving economic concern of TiO_2, various attempts have been done, and one of the most effective recent purposed solutions is combination of TiO_2 with another alternative such as SiO_2 [28], zero-valent iron (ZVI) [29], Ag [27], Cu and Au [30], and ZnO [31–33]. Compare with other NP, ZnO is more preferable because of higher performance and relatively low cost.

Design of experiment (DOE) as a collection of worthwhile mathematical techniques is applied to the statistical modeling and systematic analysis of a problem in which desired responses or output measures are optimized by input variables or factors [34, 35]. One of the numerous DOEs for empirical model building is response surface methodology (RSM) [36, 37]. The RSM method is a collection of mathematical and statistical techniques that use to develop, improve, and optimize processes and can be used for evaluation significance of several factors [38, 39]. The primary aim of RSM is determination of the optimum operational conditions for the system or specification a region ensuring the operating conditions [40, 41]. The main advantage of RSM over the conventional time-consuming approach of one factor-at-a-time (OFAT) is the reduced number of experimental runs needed for faster and more systematic investigation of the processing variables, including the simultaneous interaction of the variables and modeling of the selected response parameters [42, 43]. The central composite design (CCD) is ideal to assign the operation individual variables into a range of evaluations through the rationalized number of design points along with a reliable curvature estimation to obtain a reasonable amount of information for testing lack-of-fit (LoF) [44, 45].

To the best of our knowledge, the combination of ZnO/TiO_2 immobilized on activated carbon (AC) has not been used to As removal from water. Therefore the aims of this study are (i) to develop a novel immobilized ZnO/TiO_2 activated carbon (I ZnO/TiO_2 AC) for effective and economic arsenic removal, (ii) to investigate the effects of different variables (e.g., pH, contact time, dose) on I ZnO/TiO_2 AC system efficiency, (iii) to achieve nonlinear modeling using response surface methodology (RSM) approach, (iv) to optimize I ZnO/TiO_2 AC system for As removal from water with RSM based developed model, and finally (v) to study adsorption equilibrium isotherms by Langmuir and Freundlich models.

2 Materials and methods

2.1 Chemicals and adsorbent preparation

The whole chemicals of this study were analytical grade, and required solutions were prepared by deionized water. pH adjustment was done using 0.1 M HCl and 0.1 M NaOH which were purchased from Merck (Germany). Granular

AC (mesh = 80–100) was purchased from Jacobi carbon Company (Sweden). Arsenic trioxide (As_2O_3) 99.99% (Sigma-Aldrich, USA) was utilized for As (III) stock solution (1000 mg/L) preparation by dissolving 132 mg of its powder in 10 ml sodium hydroxide 5% which acidified with 2 ml concentrated hydrochloric acid immediately and then diluted to 100 ml with deionized water.

In order to immobilization of ZnO and TiO_2 on AC, dip-coating approach [46] was used in which $Ti(OBu)_4$ and $Zn(CH_3COO)_2 \cdot 2H_2O$ were used as precursors. TiO_2 sol was synthesized by diluting $Ti(OBu)_4$ in PrOH and adding to water dropwise under vigorous stirring (pH = 2.5 adjusted by HNO_3 purchased from Merck, Germany). The molar ratio of PrOH and water to $Ti(OBu)_4$ were 1.42 and 151, respectively. Then the solution was kept under reflux condition at 75 °C for 24 h. Eventually, PrOH and *n*-butyl alcohol removal were occurred by rotary evaporator under vacuum.

For ZnO sol preparation, first 21.90 g of $Zn(CH_3COO)_2$ was stirred in 500 ml ethanol for 30 min (water bath 50 °C), then 14.9 gr $C_6H_{15}NO_3$ was added, and stirring was continued for 1 h. After this stage heat treatment and vibration was done at 40 °C for 30 min. By adding 15 gr granular AC (GAC), vibration was continued for 30 min, and then the suspension filtered and dried. Finally calcination was done at 300 °C for 4 h. In next step TiO_2 was coated via adding previous produced ZnO/AC to 500 ml TiO_2 sol followed by vibrating (30 min), filtering, drying, and calcining at 400 °C (2 h).

2.2 Pilot specifications

The utilized experimental pilot was made from a glass cylinder with diameter = 100 mm, height = 500 mm, and total volume = 3.93 L. A cylinder made from quartz (internal and external diameter 34 mm and 36 mm, respectively) was placed in center of glass cylinder as a safety shield for ultraviolet lamp (total V = 0.51 L). After this, the final reactor effective volume was calculated to be 3.42 L. Two centrifugal pumps (Art $^{®}_{\text{Technical}}$ Co., China) were used for circulation of I ZnO/TiO_2 AC to maximize the performance of catalytic process. An ultraviolet mercury lamp (365 nm, 300 W) was placed in a quartz shield for UV resource of the reactor. The schematic of the experimental pilot was shown in Fig. 1 with detail.

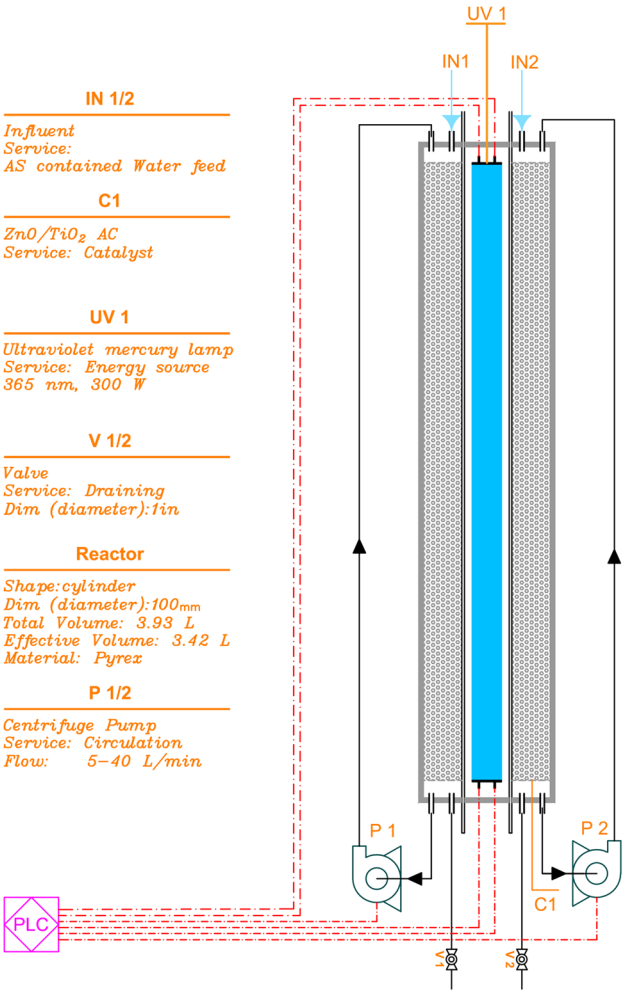

Fig. 1 Schematic of experimental pilot

2.3 Experimental design

Experimental design was consist of four numerical factors including pH (3–11), I ZnO/TiO_2 AC dose (1–3 g/L), As concentration (1–10 mg/L), and contact time (30–300 min) at three levels (− 1, 0, + 1) as well as two responses (R_1 = As removal, q_e = adsorption capacity). Thirty runs were developed using design expert software version 8 (STAT-EASE Inc., Minneapolis, USA) by using a central composite design (CCD). The second-order model (quadratic polynomial) was utilized for the prediction of responses (Eq. 1) [47–49].

$$Y = \beta_0 + \sum_{i=1}^{k} \beta_i X_i + \sum_{i=1}^{k} \beta_{ii} X_i^2 + \sum_{i=1}^{k-1} \sum_{j=i+1}^{k} \beta_{ij} X_i X_j \quad (1)$$

where β_0,β_i,β_{ii}, and β_{ij} are the regression coefficients; X_i and X_j are the independent numerical variables (coded values form); k is the total number of designed variables, and Y is the predicted response [50, 51]. The amount of As removal was calculated by Eq. 2:

$$As_R = \frac{As_{in} - As_t}{As_t} \times 100 \quad (2)$$

where As_R represented the As removal performance (%); As_{in} initial As concentration; and As_t remain As concentration after contact time. Levels of change for each variable

included central levels (0), and high and low levels of factors (+1 and − 1), which their actual values are shown in Table S1.

2.4 Analytical procedures

All of the analytical procedure was done according to the standard methods for the examination of water and wastewater handbook [52, 53]. All of the samples were filtered using filter paper (Whatman No. 42-Germany). The pH and temperature were measured by a portable pH meter (HACH-USA). The concentration of As was measured by inductively coupled plasma atomic emission spectroscopy (ICP-OES) method (SPECTRO ARCOS-Germany) at 188.98 nm. All experiments were repeated three times.

2.5 Adsorption kinetics

2.5.1 Pseudo-first-order

The pseudo-first-order kinetic model which was introduced very useful for adsorption studies by many literatures [54–56] is described as follow:

$$\ln\left[q_e - q_t\right] = \ln q_e - k_1 t \tag{3}$$

where q_e is adsorption capacity at equilibrium (mg/g), q_t is the amount of solute absorbed by adsorbent at time = t (mg/g), and k_1 is pseudo-first-order kinetic rate constant. By plotting the term of $\ln\left[q_e - q_t\right]$ versus t the amount of k_1 can be calculated [57].

2.5.2 Pseudo-second-order

The pseudo-second-order kinetic model is another popular kinetic model which was utilized widely for adsorption studies. The general equation of this model is given below (Eq. 4) [58]:

$$\frac{t}{q_t} = \frac{t}{q_e} + \frac{1}{k_2 q_e^2} \tag{4}$$

where q_e is adsorption capacity at equilibrium (mg/g), q_t is the amount of solute absorbed by adsorbent at time = t (mg/g), and k_2 is pseudo-second-order kinetic rate constant. The term of t/q_t versus t was plotted for calculation of k_2.

2.6 Adsorption equilibrium isotherms

Determination of best isotherm model which has good agreement with experimental data is one of the important factors in adsorption studies. In this study two most popular isotherms including Langmuir and Freundlich were used as follow:

2.6.1 Langmuir isotherm

The general linear equation of Langmuir isotherm [59, 60] is expressed as follows:

$$\frac{1}{q_e} = \left(\frac{1}{K_L \cdot q_{\max}}\right) \cdot \frac{1}{C_e} + \frac{1}{q_{\max}} \tag{5}$$

where q_e is adsorption capacity at equilibrium (mg/g), $q_{\max}$ is the maximum adsorption capacity (mg/g), C_e is adsorbate concentration in solution at equilibrium (mg/L), and K_L is the constant of the Langmuir isotherm (L/mg) [61].

2.6.2 Freundlich isotherm

The general linearized form of Freundlich model which was applied to describe multilayer adsorption over the heterogeneous surface by many literatures [55, 56, 59, 62] is given below:

$$\ln q_e = \ln K_F + (1/n) \ln C_e \tag{6}$$

where q_e is adsorption capacity at equilibrium (mg/g), C_e is adsorbate concentration in solution at equilibrium (mg/L), and K_F is the constant of the Freundlich isotherm $(mg/g)/(mg/L)^{1/n}$; n is the Freundlich adsorption validity indicator, when the value of $(1/n)$ ranged between 0 and 1 represent an appropriate adsorption by Freundlich isotherm. The chemisorption is happen when $(1/n < 0)$, and the Langmuir isotherm is favorable when $(n = 0)$. Plotting $\ln q_e$ versus $\ln C_e$ demonstrates a straight line which the slope and intercept represent $1/n$ and K_F, respectively [63, 64]. To give greater insight into the CCD results, Pareto analysis was used to calculate the percentage effect of each independent variable (P_i) on the removal of As (Eq. 7) [65–67]:

$$P_i = \left(\frac{\beta_i^2}{\sum \beta_i^2}\right) \times 100 \quad i \neq 0 \tag{7}$$

3 Results and discussion

3.1 XRD and SEM analyzes

Scanning electron microscope (SEM) of the prepared I ZnO/TiO_2 AC is presented at Fig. 2a. As can be seen clearly in the colorful section of the image, the ZnO/TiO_2 nanoparticles were regularly dispersed on AC. It also shows ZnO and TiO_2 were covered most surface of the AC which increase the catalytic activity of I ZnO/TiO_2 AC due to good interaction with UV. The black and white section of the image is showing the morphology, pour, and particle sizes as well as overall situation of the lab synthesized I-ZnO/TiO_2 AC. It clearly shows that I-ZnO/TiO_2 AC have different morphology,

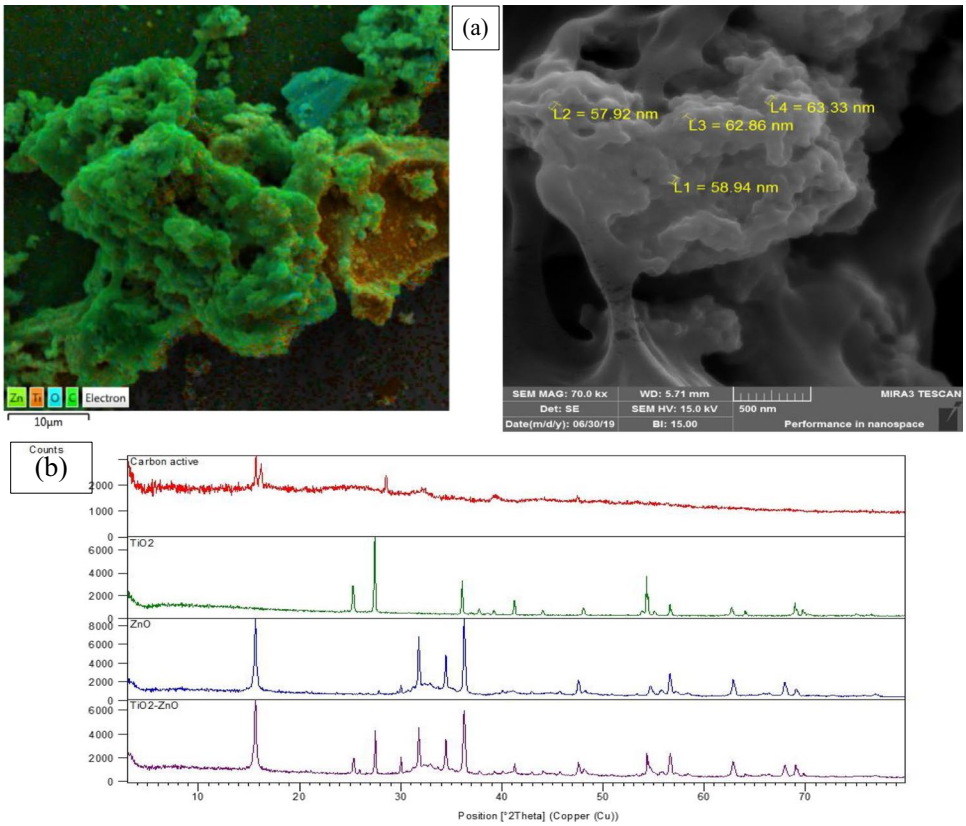

Fig. 2 **a** Scanning electron microscope (SEM) of the prepared I ZnO/TiO_2 AC, **b** X-Ray diffraction comparison of AC, TiO_2, ZnO, I ZnO/TiO_2 AC

shape, and sizes which make a heterogeneous photocatalytic adsorbent. In addition it can verify that particles size are ranged between 57.92 and 63.33 nm (nm) so the structure of particles are confirmed as nanoscale (< 100 nm).

The structure of the prepared I-ZnO/TiO_2 AC was studied by XRD analyzes (CuKα and λ = 1.54060 Å). Figure 2b shows the XRD pattern and main peaks of rutile phase at 2θ including 27.44° (110), 36.07° (011), 39.20° (020), 41.24° (111), 44.05° (120), 54.32° (121), 56.64° (220), 62.72° (002), 64.06° (130), 69.01° (031), and 69.78° (112). It also shows the peaks of anatase phase at 2θ including; 25.31 (011), 37.75 (004), 48.06 (020), 53.86° (015), and 55.08° (121).

From the XRD pattern, it is quite clear that the main peaks of 31.80° (010), 34.46° (002), 36.29° (011), 47.57° (012), 56.62° (110), 62.88° (013), 67.96° (112), and 69.10° (021) at 2θ are confirming the presence of ZnO on the prepared adsorbent. The above mentioned facts revealed that the lab synthesized I-ZnO/TiO_2 AC contain standard ZnO and TiO_2.

3.2 Experimental modeling analysis

The designed experiments including factors and obtained responses are summarized in Table 1. In order to determine the regression model of As removal by I ZnO/TiO_2 AC, a quadratic model was utilized to find out the relationship between independent numerical variables and predicted responses. Central composite design was developed this relationship as follows:

$$\begin{aligned} \text{As } R = {} & 92.0366 + 4.2083\ A - 1.0433\ B \\ & + 27.2078\ C - 8.415\ D - 0.5287\ AB \\ & + 0.3212\ AC + 0.1925\ AD + 0.1550\ BC \\ & + 0.0812\ BD + 4.9762\ CD - 5.1598\ A^2 \\ & - 8.7748\ B^2 - 17.6548\ C^2 + 0.3502\ D^2 \end{aligned} \quad (8)$$

$$\begin{aligned} \text{As } R = {} & -3.5414 + 25.145\ D + 7.6093\ pH \\ & + 0.4694\ T - 3.5289\ C - 0.1321\ D \times pH \\ & + 0.0024\ D \times T + 0.0428\ D \times C \\ & + 0.0003\ pH \times T + 0.0045\ pH \times C \\ & + 0.0082\ T \times C - 5.1598\ D^2 - 0.5484\ pH^2 \\ & - 0.0010\ T^2 + 0.0173\ C^2 \end{aligned} \quad (9)$$

which Eq. 8 is based on coded factor (the high levels of the factors are coded as + 1 and the low levels of the factors are coded as − 1) and Eq. 9 is based on actual factor so it can be used to make predictions about the responses for given levels of each factor. In Eq. 8, A, B, C, and D represent the nano absorbent dose, pH, contact time, and As concentration,

Table 1 Experimental design and responses

Runs	Coded values				Un-coded values				Responses	
	X_1	X_2	X_3	X_4	D (g/L)[a]	pH	CT (min)	C (mg/L)	R_1	R_2
1	0	0	0	0	2	7	165	5.5	92.73	2.55
2	−1	1	1	1	1	11	300	10	80.97	8.09
3	−1	0	0	0	1	7	165	5.5	82.32	4.52
4	0	0	−1	0	2	7	30	5.5	46.96	1.29
5	0	0	1	0	2	7	300	5.5	100	2.75
6	1	−1	1	1	3	3	300	10	91.74	3.06
7	−1	1	−1	−1	1	11	30	1	42.16	0.42
8	1	−1	−1	1	3	3	30	10	25.87	0.86
9	1	4	−1	−1	3	11	30	1	48.81	0.16
10	−1	−1	1	−1	1	3	300	1	87.13	0.87
11	−1	−1	−1	1	1	3	30	10	16.34	1.63
12	-1	1	1	−1	1	11	300	1	86.43	0.86
13	1	1	1	−1	3	11	300	1	95.39	0.32
14	0	0	0	0	2	7	165	5.5	93.46	2.57
15	−1	−1	1	1	1	3	300	10	79.89	7.99
16	0	0	0	0	2	7	165	5.5	93.61	2.57
17	−1	1	−1	1	1	11	30	10	14.95	1.49
18	0	0	0	0	2	7	165	5.5	91.94	2.53
19	1	−1	−1	−1	3	3	30	1	51.82	0.17
20	1	1	−1	1	3	11	30	10	23.79	0.79
21	1	0	0	0	3	7	165	5.5	89.63	1.64
22	0	1	0	0	2	11	165	5.5	81.24	2.23
23	0	−1	0	0	2	3	165	5.5	83.48	2.29
24	1	1	1	1	3	11	300	10	86.51	2.88
25	0	0	0	−1	2	7	165	1	100	0.50
26	0	0	0	1	2	7	165	10	82.97	4.15
27	1	−1	1	−1	3	3	300	1	97.57	0.32
28	0	0	0	0	2	7	165	5.5	94.02	2.58
29	0	0	0	0	2	7	165	5.5	91.87	2.53
30	−1	−1	−1	−1	1	3	30	1	45.19	0.45

[a]*D* I ZnO/TiO_2 AC dosage; *CT* contact time; *C* As initial concentration; R_1 As removal (%); R_2 adsorption capacity (mg/g)

respectively. The amount of *F* value (=822.68) indicate the model is significant. There is only a 0.01% chance that an *F* value this large could occur due to noise. The *P* values less than 0.05 in each terms demonstrate model terms are significant, and greater than 0.1 indicate the model terms are not significant (A, B, C, D, CD, A^2, B^2, and C^2 were obtained as the significant model terms). All of these findings refer to appropriate model which was developed. Additional information About analyses of ANOVA are summarized in Table 2. As can easily understand from this table the amount of predicted R-squared of 0.9938 is in reasonable agreement with the adjusted R-squared of 0.9975 (difference < 0.2). The signal to noise ratio of 89.608 (> 4) means it is adequate signal so this model can be used to navigate the design space. Figure S1 shows the Pareto graphic analysis. The results of Fig. S1 suggest that among the variables, contact time (C)

Table 2 Summary of model statically analyses

Parameter	As removal	q_e
Sum of squares	21,246.67	30.97
df	14	14
Mean square	1517.62	2.21
F value	822.68	291.96
P value Prob > F	< 0.0001 (significant)	< 0.0001 (significant)
Std. Dev	1.36	0.09
Mean	73.29	0.34
R-squared	0.9987	0.9963
Adj R-squared	0.9975	0.9929
Pred R-squared	0.9938	0.9806
Adeq Precision	89.6080	62.4704

Table 3 Final selected solution for meeting requirement

Number	D (g/L)	pH	T (min)	C (mg/L)	As R (%)	q_e (mg/g)	Desirability	Result
1	2.456	6.756	287.570	9.768	99.900	4.365	0.996	Selected

variable was the most important factor for As removal with 34.49%. The lack of fit (LoF) which compares residual error with pure error was also checked and shown to be not significant in comparison with pure error. In our present study with regard to As removal onto used adsorption process, the LOF is not significant relative to the pure error, indicating good response to the model (P value > 0.05). A desirable R^2 value is close to 1, and a reasonable agreement with adjusted R^2 is necessary. As can be seen from results, the model regression coefficient ($R^2 = 0.9987$) shows that 99.87% of variability in As removal can be explained by the predicted model and is left with 0.13% residual variability. Furthermore, in present study for As removal, the predicted R^2 of (0.9938) is in reasonable agreement with the adjusted R^2 of (00.9975). To survey the ability of models among various models (linear, 2FI, quadratic, and cubic), the sequential model sum of squares was performed. The adequate model for removal efficiency of As was selected by the probability value ($P < 0.05$) and the Fisher's F value along with the determination of coefficient (R^2). The fit summary for removal efficiency of As suggested a quadratic relationship, where the additional terms were significant and the model was not aliased. Residuals plots describe the difference between the observed values of a response and its predicted value and are essential to estimate the adequacy of the model. Normal test plots are graphical tools for signifying the residuals departure from a straight line. The normal probability plot of As removal using adsorption process (Fig. S1a show that almost all data points are normally scattered near to the straight line and there is no gross distribution around the line. The adequacy of the model was also evaluated by the plot of residuals versus the predicted responses. Figure S1b disclosed that the random scatter of the residuals around the zero denotes the proper behavior of the models and the gratification of constant variance assumptions. Furthermore, in a well-designed model, the residuals should be independent of time or any other parameters. In the represented externally studentized residuals versus run (Fig. S1c), any observable trend demonstrates independency of the residuals to the runs. In general, the proposed model was adequately able to predict the removal of As by adsorption process.

3.3 Optimization of process

After modeling step finding optimized criteria for As removal in maximum concentration was carried out with emphasize on meeting standard regulations. According to Environmental Protection Agency (EPA) maximum contaminant level (MCL) of 10 µg/L is acceptable for drinking water [68]. The final appropriate solution which was selected by developed response surface model is presented in Table 3. It demonstrated that the best dosage, pH, T, and initial concentration to reach permitted concentration for output (10 µg/L) are 2.456 g/L, 6.756, 287.570 min, and 9.768 mg/L, respectively. The appropriate achieved desirability (0.996) depicted that the solution is acceptable (also the agreement of predicted and actual values in Fig. 3). Similar findings were reported by Tsimas et al. (2009) (pH = 6.4) [69].

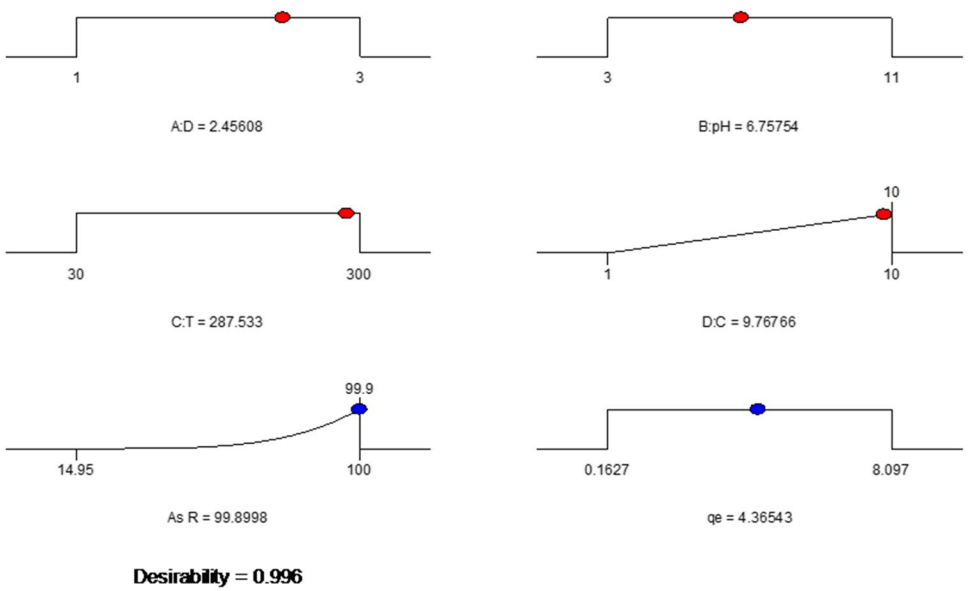

Fig. 3 The amount of actual versus predicted values

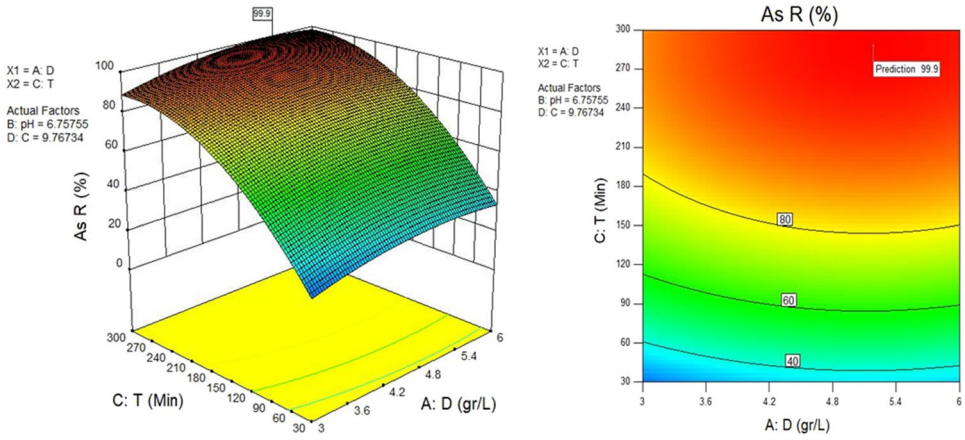

Fig. 4 The amount of actual versus predicted values effect of contact time and I ZnO/TiO_2 AC dosage on AS removal

3.4 Performance evaluation

Effects of various criteria on As removal are shown in Fig. 4. Figure 4 illustrates effect of contact time and I ZnO/TiO_2 AC dosage on As removal and q_e in optimized condition (actual factor: D = 5.18741 g/L and pH = 6.75755). There is a direct relationship between increases in contact time and decreases in As concentration and system performance. Minimum removal efficiency of 14.95% was obtained for T = 30 min and C = 10 mg/L. This was probably done due to the required time for oxidation of As. Tsimas et al. (2009) were reported that 30 min reaction time is needed for completely As oxidation with initial concentration of 10 mg/L [69]. So after oxidation of As, the adsorption rate was increased with T which 99.90% of As was removed at T = 287.6 min C = 9.8 mg/L. Figure 5 was plotted for evaluation of simultaneous effect of contact time and pH on As removal (actual factor: D = 5.18741 g/L and C = 9.76734). From the figure it can easily understand that the best performance was achieved in pH = 6.8 and also depict the drop in performance as any decrease or increase in pH. Similar behavior was observed by Altundogan et al. (2000) [70]. This phenomenon is expected due to point of zero charge (pH_{pzc}) of both nanoparticles. The pH_{pzc} of TiO_2 was ranged between 4.5 and 6.1 according to previous literature, and this amount was reported 6.9 for ZnO. Based on previous studies, ZnO effectively works in the pH range of 5.8–6.8, and these findings are in accordance of our results (Singh et al., 2012). Figure 6 demonstrates effect of contact time and As initial concentration on As removal in which as we expected the performance was dramatically decreased by increasing the As concentration (14.95–100%).

3.5 Adsorption kinetics and isotherm

After finding the optimized points, the kinetic analyses of As removal was studied, and the results are summarized in Fig. 7. According to Fig. 7a, the equilibrium time and q_e were 250 min and 3.896, respectively. Figure 7b was plotted for pseudo-first-order kinetic model and the result demonstrated that the obtained data have good agreement with this model ($R^2 = 0.9749$). Figure 7c was obtained using pseudo-second-order kinetic model, and the correlation

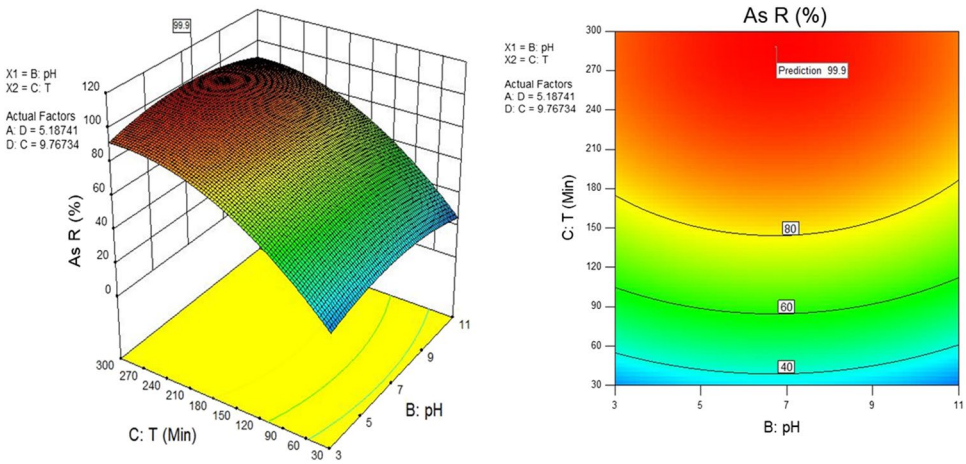

Fig. 5 Effect of contact time and pH on As removal

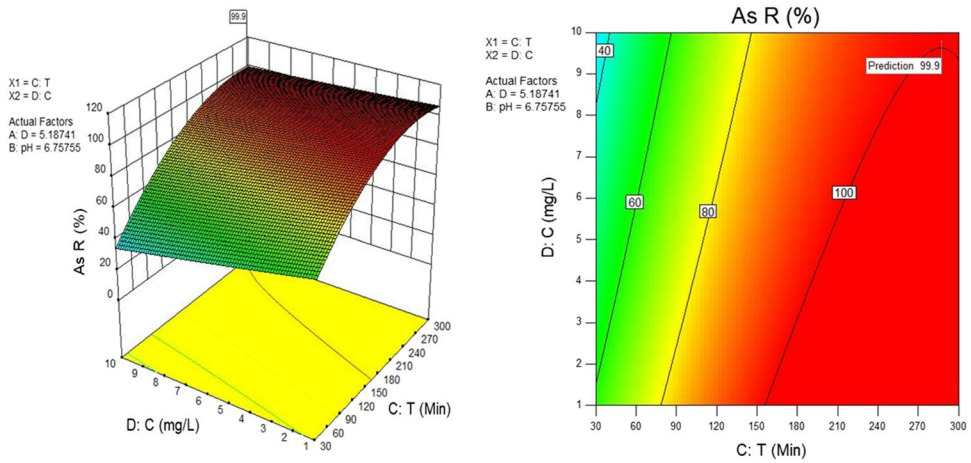

Fig. 6 Effect of contact time and As initial concentration on As removal

coefficient ($R^2 = 0.9995$) depicted this model has better agreement with the experimental data. Figures 7d and e were plotted for the appropriate isotherm for adsorption analyses. The result showed that the Langmuir isotherm has better agreement with the obtained data.

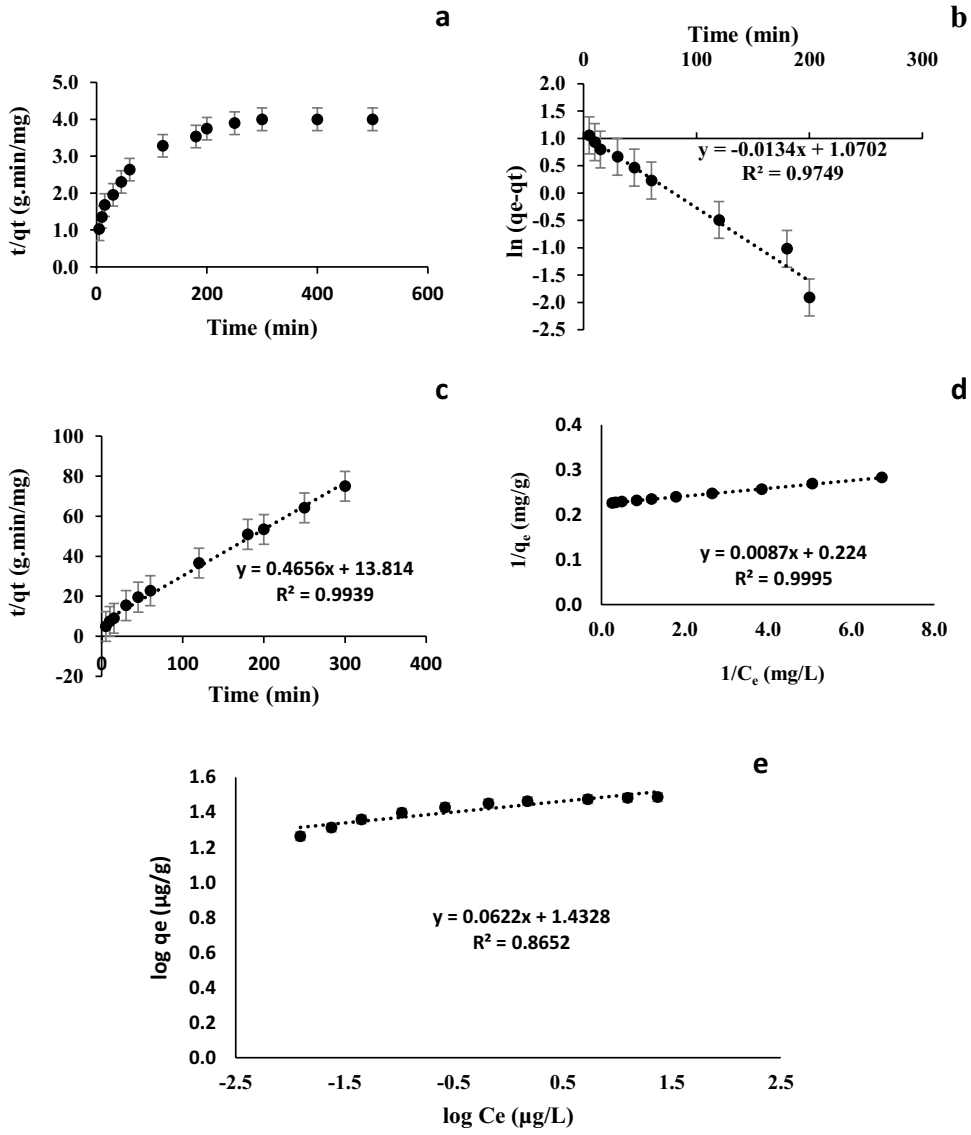

Fig. 7 Kinetic analysis of AS removal by I ZnO/TiO_2 AC

4 Conclusion

An immobilized ZnO/TiO_2 activated carbon (nanoscale) was developed to arsenic removal from water and was modeled by response surface modeling approach to find the optimized condition. According to obtained results, the best dosage, pH, T, and concentration to meet environmental requirements are 5.187 g/L, 6.758, 287.574 min, and 9.767 mg/L, respectively. The evaluation of obtained model was showed that the model is appropriate to use for performance prediction of the system. Finally, it can be concluded that the novel immobilized ZnO/TiO_2 activated carbon have a very high performance in As removal along with economic it manner, so it is seriously purposeful for practical use.

Supplementary Information The online version contains supplementary material available at https://doi.org/10.1007/s13399-021-01741-1.

Author contribution Nastuna Ghanbari Sagharloo: conceptualization, methodology, validation, formal analysis, investigation, resources, supervision, funding acquisition. Mohammad rabani: methodology; validation; resources; writing, original draft; writing, review and editing. Lida salimi: analyses, writing and text revision. Hossein Ghafourian and S.M.T Sadatipour: methodology, validation, formal analysis, investigation.

Funding The current study was financially supported by Tehran North Branch, Islamic Azad University, Tehran, Iran.

Data availability The dataset and analyzed during the current study are available from the corresponding authors on realistic demand.

Declarations

Ethics approval and consent to participate Not applicable.

Consent for publication Not applicable.

Conflict of interest The authors declare no competing interests.

References

1. Pirsaheb M, Ejraei A (2016) Evaluating the performance of inorganic coagulants (Poly aluminum chloride, ferrous sulfate, ferric chloride and aluminum sulfate) in removing the turbidity from aqueous solutions. Int J Pharm Technol 8:13168–13181
2. Shokoohi R, Movahedian H, Dargahi A, Jafari AJ, Parvaresh A (2017) Survey on efficiency of BF/AS integrated biological system in phenol removal of wastewater. Desalin Water Treat 82:315–321
3. Samarghandi MR, Mohammadi M, Karami A, Tabandeh L, Dargahi A, Amirian F (2017) Residue analysis of pesticides, herbicides, and fungicides in various water sources using gas chromatography-mass detection. Pol J Environ Stud 26:2189–2195
4. Alalwan HA, Kadhom MA, Alminshid AH (2020) Removal of heavy metals from wastewater using agricultural byproducts. J Water Supply Res Technol AQUA 69:99–112
5. Dargahi A, Golestanifar H, Darvishi P, Karam A (2016) An investigation and comparison of removing heavy metals (lead and chromium) from aqueous solutions using magnesium oxide nanoparticles. Pol J Environ Stud 25:557–562
6. Almasi A, Dargahi A, Ahagh M, Janjani H, Mohammadi M, Tabandeh L (2016) Efficiency of a constructed wetland in controlling organic pollutants, nitrogen, and heavy metals from sewage. J Chem Pharm Sci 9:2924–2928
7. Ociński D, Jacukowicz-Sobala I, Mazur P, Raczyk J, Kociołek-Balawejder E (2016) Water treatment residuals containing iron and manganese oxides for arsenic removal from water–characterization of physicochemical properties and adsorption studies. Chem Eng J 294:210–221
8. Ahoranta SH, Kokko ME, Papirio S, Özkaya B, Puhakka JA (2016) Arsenic removal from acidic solutions with biogenic ferric precipitates. J Hazard Mater 306:124–132
9. Wang J, Xu W, Chen L, Huang X, Liu J (2014) Preparation and evaluation of magnetic nanoparticles impregnated chitosan beads for arsenic removal from water. Chem Eng J 251:25–34
10. Abejón A, Garea A, Irabien A (2015) Arsenic removal from drinking water by reverse osmosis: minimization of costs and energy consumption. Sep Purif Technol 144:46–53
11. Kumar PR, Chaudhari S, Khilar KC, Mahajan S (2004) Removal of arsenic from water by electrocoagulation. Chemosphere 55:1245–1252
12. Lee C-G, Alvarez PJ, Nam A, Park S-J, Do T, Choi U-S, Lee S-H (2017) Arsenic (V) removal using an amine-doped acrylic ion exchange fiber: kinetic, equilibrium, and regeneration studies. J Hazard Mater 325:223–229
13. Xie L, Liu P, Zheng Z, Weng S, Huang J (2016) Morphology engineering of V2O5/TiO2 nanocomposites with enhanced visible light-driven photofunctions for arsenic removal. Appl Catal B 184:347–354
14. Samad A, Furukawa M, Katsumata H, Suzuki T, Kaneco S (2016) Photocatalytic oxidation and simultaneous removal of arsenite with CuO/ZnO photocatalyst. J Photochem Photobiol, A 325:97–103
15. Afsharnia M, Kianmehr M, Biglari H, Dargahi A, Karimi A (2018) Disinfection of dairy wastewater effluent through solar photocatalysis processes. Water Sci Eng 11:214–219
16. Carolin CF, Kumar PS, Saravanan A, Joshiba GJ, Naushad M (2017) Efficient techniques for the removal of toxic heavy metals from aquatic environment: a review. J Environ Chem Eng 5:2782–2799
17. Mohanty D (2017) Conventional as well as emerging arsenic removal technologies—a critical review. Water Air Soil Pollut 228:381
18. Phanthasri J, Khamdahsag P, Jutaporn P, Sorachoti K, Wantala K, Tanboonchuy V (2018) Enhancement of arsenite removal using manganese oxide coupled with iron (III) trimesic. Appl Surf Sci 427:545–552
19. Vaiano V, Iervolino G, Rizzo L (2018) Cu-doped ZnO as efficient photocatalyst for the oxidation of arsenite to arsenate under visible light. Appl Catal B 238:471–479
20. Samarghandi MR, Dargahi A, Zolghadr Nasab H, Ghahramani E, Salehi S (2020) Degradation of azo dye Acid Red 14 (AR14) from aqueous solution using H2O2/nZVI and S2O82–/nZVI processes in the presence of UV irradiation. Water Environ Res 92(8):1173–1183
21. Molinari R, Argurio P (2017) Arsenic removal from water by coupling photocatalysis and complexation-ultrafiltration processes: a preliminary study. Water Res 109:327–336
22. Guan X, Du J, Meng X, Sun Y, Sun B, Hu Q (2012) Application of titanium dioxide in arsenic removal from water: a review. J Hazard Mater 215:1–16
23. Nakajima T, Xu Y-H, Mori Y, Kishita M, Takanashi H, Maeda S, Ohki A (2005) Combined use of photocatalyst and adsorbent for the removal of inorganic arsenic (III) and organoarsenic compounds from aqueous media. J Hazard Mater 120:75–80

24. Zhang F-S, Itoh H (2006) Photocatalytic oxidation and removal of arsenite from water using slag-iron oxide-TiO2 adsorbent. Chemosphere 65:125–131
25. Xu Z, Meng X (2009) Size effects of nanocrystalline TiO2 on As (V) and As (III) adsorption and As (III) photooxidation. J Hazard Mater 168:747–752
26. Souza RP, Freitas TK, Domingues FS, Pezoti O, Ambrosio E, Ferrari-Lima AM, Garcia JC (2016) Photocatalytic activity of TiO2, ZnO and Nb2O5 applied to degradation of textile wastewater. J Photochem Photobiol, A 329:9–17
27. Kanakaraju D, Kockler J, Motti CA, Glass BD, Oelgemöller M (2015) Titanium dioxide/zeolite integrated photocatalytic adsorbents for the degradation of amoxicillin. Appl Catal B 166:45–55
28. Bo Zhong J, Zhang Li J, Mei Feng F, Lu Y, Zeng J, Hu W, Tang Z (2012) Improved photocatalytic performance of SiO2–TiO2 prepared with the assistance of SDBS. J Mol Catal A Chem 357:101–105
29. Hsieh W-P, Pan JR, Huang C, Su Y-C, Juang Y-J (2010) Enhance the photocatalytic activity for the degradation of organic contaminants in water by incorporating TiO2 with zero-valent iron. Sci Total Environ 408:672–679
30. Manzoli M, Chiorino A, Boccuzzi F (2005) Decomposition and combined reforming of methanol to hydrogen: a FTIR and QMS study on Cu and Au catalysts supported on ZnO and TiO2. Appl Catal B 57:201–209
31. Filipe P, Silva J, Silva R, De Castro JC, Gomes MM, Alves L, Santus R, Pinheiro T (2009) Stratum corneum is an effective barrier to TiO2 and ZnO nanoparticle percutaneous absorption. Skin Pharmacol Physiol 22:266–275
32. Liao S, Donggen H, Yu D, Su Y, Yuan G (2004) Preparation and characterization of ZnO/TiO2, SO42−/ZnO/TiO2 photocatalyst and their photocatalysis. J Photochem Photobiol, A 168:7–13
33. Wang J, Li J, Xie Y, Li C, Han G, Zhang L, Xu R, Zhang X (2010) Investigation on solar photocatalytic degradation of various dyes in the presence of Er3+: YAlO3/ZnO–TiO2 composite. J Environ Manag 91:677–684
34. Hasani K, Moradi M, Mokhtari SA, Dargahi A, Vosoughi M (2021) Degradation of basic violet 16 dye by electro-activated persulfate process from aqueous solutions and toxicity assessment using microorganisms: determination of by-products, reaction kinetic and optimization using Box-Behnken design. Int J Chem Reactor Eng 19:261–275
35. Almasi A, Mahmoudi M, Mohammadi M, Dargahi A, Biglari H (2021) Optimizing biological treatment of petroleum industry wastewater in a facultative stabilization pond for simultaneous removal of carbon and phenol. Toxin Rev 40:189–197
36. Dargahi A, Ansari A, Nematollahi D, Asgari G, Shokoohi R, Samarghandi MR (2019) Parameter optimization and degradation mechanism for electrocatalytic degradation of 2, 4-dicloro-phenoxyacetic acid (2, 4-D) herbicide by lead dioxide electrodes. RSC Adv 9:5064–5075
37. Rahmani A, Salari M, Tari K, Shabanloo A, Shabanloo N, Bajalan S (2020) Enhanced degradation of furfural by heat-activated persulfate/nZVI-rGO oxidation system: Degradation pathway and improving the biodegradability of oil refinery wastewater. J Environ Chem Eng 8:104468
38. Dargahi A, Mohammadi M, Amirian F, Karami A, Almasi A (2017) Phenol removal from oil refinery wastewater using anaerobic stabilization pond modeling and process optimization using response surface methodology (RSM). Desalin Water Treat 87:199–208
39. Rahmani A, Seid-Mohammadi A, Leili M, Shabanloo A, Ansari A, Alizadeh S, Nematollahi D (2021) Electrocatalytic degradation of diuron herbicide using three-dimensional carbon felt/β-PbO2 anode as a highly porous electrode: influencing factors and degradation mechanisms. Chemosphere 276:130141
40. Azizi A, Dargahi A, Almasi A (2019) Biological removal of diazinon in a moving bed biofilm reactor–process optimization with central composite design. Toxin Rev 1–11
41. Almasi A, Dargahi A, Mohammadi M, Azizi A, Karami A, Baniamerian F, Saeidimoghadam Z (2016) Application of response surface methodology on cefixime removal from aqueous solution by ultrasonic/photooxidation. Int J Pharm Technol 8:16728–16736
42. Heidari M, Vosoughi M, Sadeghi H, Dargahi A, Mokhtari SA (2020) Degradation of diazinon from aqueous solutions by electro-Fenton process: effect of operating parameters, intermediate identification, degradation pathway, and optimization using response surface methodology (RSM). Sep Sci Technol 1–13
43. Shokoohi R, Jafari AJ, Dargahi A, Torkshavand Z (2017) Study of the efficiency of bio-filter and activated sludge (BF/AS) combined process in phenol removal from aqueous solution: determination of removing model according to response surface methodology (RSM). Desalin Water Treat 77:256–263
44. Alizadeh S, Sadeghi H, Vosoughi M, Dargahi A, Mokhtari SA (2020) Removal of humic acid from aqueous media using sono-persulphate process: optimization and modelling with response surface methodology (RSM). Int J Environ Anal Chem 1–15
45. Molla Mahmoudi M, Khaghani R, Dargahi A, Monazami Tehrani G (2020) Electrochemical degradation of diazinon from aqueous media using graphite anode: effect of parameters, mineralisation, reaction kinetic, degradation pathway and optimisation using central composite design. Int J Environ Anal Chem 1–26
46. Hu Y, Yuan C (2006) Low-temperature preparation of photocatalytic TiO 2 thin films on polymer substrates by direct deposition from anatase sol. Cailiao Kexue Yu Jishu (J Mater Sci Technol) 22:239–244
47. Samarghandi MR, Dargahi A, Rahmani A, Shabanloo A, Ansari A, Nematollahi D (2021) Application of a fluidized three-dimensional electrochemical reactor with Ti/SnO2–Sb/β-PbO2 anode and granular activated carbon particles for degradation and mineralization of 2, 4-dichlorophenol: process optimization and degradation pathway. Chemosphere 279:130640
48. Afshin S, Rashtbari Y, Vosough M, Dargahi A, Fazlzadeh M, Behzad A, Yousefi M (2021) Application of Box-Behnken design for optimizing parameters of hexavalent chromium removal from aqueous solutions using Fe3O4 loaded on activated carbon prepared from alga: kinetics and equilibrium study. J Water Process Eng 42:102113
49. Samarghandi MR, Dargahi A, Shabanloo A, Nasab HZ, Vaziri Y, Ansari A (2020) Electrochemical degradation of methylene blue dye using a graphite doped PbO2 anode: optimization of operational parameters, degradation pathway and improving the biodegradability of textile wastewater. Arab J Chem 13:6847–6864
50. Samarghandi MR, Nemattollahi D, Asgari G, Shokoohi R, Ansari A, Dargahi A (2019) Electrochemical process for 2, 4-D herbicide removal from aqueous solutions using stainless steel 316 and graphite anodes: optimization using response surface methodology. Sep Sci Technol 54:478–493
51. Hasani K, Peyghami A, Moharrami A, Vosoughi M, Dargahi A (2020) The efficacy of sono-electro-Fenton process for removal of cefixime antibiotic from aqueous solutions by response surface methodology (RSM) and evaluation of toxicity of effluent by microorganisms. Arab J Chem 13:6122–6139
52. Dargahi A, Hasani K, Mokhtari SA, Vosoughi M, Moradi M, Vaziri Y (2021) Highly effective degradation of in a three-dimensional sono-electro-Fenton (3D/SEF) system using powder activated carbon (PAC)/Fe3O4 as magnetic particle electrode. J Environ Chem Eng 105889
53. Dargahi A, Nematollahi D, Asgari G, Shokoohi R, Ansari A, Samarghandi MR (2018) Electrodegradation of 2, 4-dichlorophenoxyacetic acid herbicide from aqueous solution using

three-dimensional electrode reactor with G/β-PbO 2 anode: Taguchi optimization and degradation mechanism determination. RSC Adv 8:39256–39268
54. Simonin J-P (2016) On the comparison of pseudo-first order and pseudo-second order rate laws in the modeling of adsorption kinetics. Chem Eng J 300:254–263
55. Dargahi A, Samarghandi MR, Shabanloo A, Mahmoudi MM, Nasab HZ (2021) Statistical modeling of phenolic compounds adsorption onto low-cost adsorbent prepared from aloe vera leaves wastes using CCD-RSM optimization: effect of parameters, isotherm, and kinetic studies. Biomass Conver Bioref 1–5. https://doi.org/10.1007/s13399-021-01601-y
56. Mouni L, Belkhiri L, Bollinger J-C, Bouzaza A, Assadi A, Tirri A, Dahmoune F, Madani K, Remini H (2018) Removal of methylene blue from aqueous solutions by adsorption on Kaolin: kinetic and equilibrium studies. Appl Clay Sci 153:38–45
57. Seid-Mohammadi A, Asgarai G, Ghorbanian Z, Dargahi A (2020) The removal of cephalexin antibiotic in aqueous solutions by ultrasonic waves/hydrogen peroxide/nickel oxide nanoparticles (US/H2O2/NiO) hybrid process. Sep Sci Technol 55:1558–1568
58. Shokoohi R, Dargahi A, Gilan RA, Nasab HZ, Zeynalzadeh D, Mahmoudi MM (2019) Magnetic multi-walled carbon nanotube as effective adsorbent for ciprofloxacin (CIP) removal from aqueous solutions: isotherm and kinetics studies. Int J Chem Reactor Eng 18(2):1–15
59. Chung H-K, Kim W-H, Park J, Cho J, Jeong T-Y, Park P-K (2015) Application of Langmuir and Freundlich isotherms to predict adsorbate removal efficiency or required amount of adsorbent. J Ind Eng Chem 28:241–246
60. Samarghandi M, Rahmani A, Asgari G, Ahmadidoost G, Dargahi A (2018) Photocatalytic removal of cefazolin from aqueous solution by AC prepared from mango seed+ ZnO under uv irradiation. Glob NEST J 20:399–407
61. Samarghandi MR, Asgari G, Shokoohi R, Dargahi A, Arabkouhsar A (2019) Removing amoxicillin antibiotic from aqueous solutions by Saccharomyces cerevisiae bioadsorbent: kinetic, thermodynamic and isotherm studies. Desalin Water Treat 152:306–315
62. Seidmohammadi A, Vaziri Y, Dargahi A, Nasab HZ (2021) Improved degradation of metronidazole in a heterogeneous photo-Fenton oxidation system with PAC/Fe3O4 magnetic catalyst: biodegradability, catalyst specifications, process optimization, and degradation pathway. Biomass Conver Bioref 1–7. https://doi.org/10.1007/s13399-021-01668-7
63. Mahmoudi MM, Nasseri S, Mahvi AH, Dargahi A, Khubestani MS, Salari M (2019) Fluoride removal from aqueous solution by acid-treated clinoptilolite: isotherm and kinetic study. Desalin Water Treat 146:333–340
64. Shokoohi R, Gillani RA, Mahmoudi MM, Dargahi A (2018) Investigation of the efficiency of heterogeneous Fenton-like process using modified magnetic nanoparticles with sodium alginate in removing Bisphenol A from aquatic environments: kinetic studies. Desalin Water Treat 101:185–192
65. Rahmani AR, Salari M, Shabanloo A, Shabanloo N, Bajalan S, Vaziri Y (2020) Sono-catalytic activation of persulfate by nZVI-reduced graphene oxide for degradation of nonylphenol in aqueous solution: process optimization, synergistic effect and degradation pathway. J Environ Chem Eng 8:104202
66. Shokoohi R, Bajalan S, Salari M, Shabanloo A (2019) Thermochemical degradation of furfural by sulfate radicals in aqueous solution: optimization and synergistic effect studies. Environ Sci Pollut Res 26:8914–8927
67. Dargahi A, Shokoohi R, Asgari G, Ansari A, Nematollahi D, Samarghandi MR (2021) Moving-bed biofilm reactor combined with three-dimensional electrochemical pretreatment (MBBR–3DE) for 2, 4-D herbicide treatment: application for real wastewater, improvement of biodegradability. RSC Adv 11:9608–9620
68. Powers M, Yracheta J, Harvey D, O'Leary M, Best LG, Bear AB, MacDonald L, Susan J, Hasan K, Thomas E (2019) Arsenic in groundwater in private wells in rural North Dakota and South Dakota: water quality assessment for an intervention trial. Environ Res 168:41–47
69. Tsimas ES, Tyrovola K, Xekoukoulotakis NP, Nikolaidis NP, Diamadopoulos E, Mantzavinos D (2009) Simultaneous photocatalytic oxidation of As (III) and humic acid in aqueous TiO2 suspensions. J Hazard Mater 169:376–385
70. Altundoğan HS, Altundoğan S, Tümen F, Bildik M (2000) Arsenic removal from aqueous solutions by adsorption on red mud. Waste Manag 20:761–767